

Experimental report

28/01/2021

Proposal: 7-05-508

Council: 4/2019

Title: How does tuning the van der Waals bonding strength affect adsorbate structure and nanoscale diffusion?

Research area: Physics

This proposal is a new proposal

Main proposer: Anton TAMTOEGL

Experimental team: Peter FOUQUET
Anton TAMTOEGL
Chris TRUSCOTT
Nadav AVIDOR

Local contacts: Thomas HANSEN
Michael Marek KOZA

Samples: C₄H₄N₂/graphite
C₄D₄N₂/graphite

Instrument	Requested days	Allocated days	From	To
D20	3	2	04/02/2020	06/02/2020
IN6-SHARP	5	3	06/09/2019	09/09/2019

Abstract:

We plan to characterise the effect of van-der-Waals (vdW) interactions between heterocyclic analogues of benzene and graphite on the surface adsorption structure and diffusion process. Therefore we propose to measure the structure and diffusion of pyrazine (C₄H₄N₂) on exfoliated graphite.

By substituting nitrogen atoms into the ring of aromatic hydrocarbons the electronic density around the carbon atoms of the molecule is reduced, giving rise to a stronger bonding with the substrate via tuning of the vdW interaction. Hence, by systematically changing the interaction strength with the substrate, these experiments will allow us to elucidate the influence of the vdW interaction strength on the adsorption structure and the nanoscale diffusion process. The latter includes different aspects of energy dissipation in surface diffusion, in particular the contribution of electronic friction.

How does tuning the van der Waals bonding strength affect adsorbate structure and nanoscale diffusion? (7-05-508)

A. Tamtögl,^{*,†} C. Truscott,[‡] N. Avidor,[¶] M. Sacchi,[§] M. M. Koza,^{||} P. Fouquet,^{||} and T. C. Hansen^{||}

[†]*Institute of Experimental Physics, Graz University of Technology, Graz, Austria*

[‡]*Department of Chemistry, University of Cambridge, Lensfield Road, Cambridge CB2 1EW, United Kingdom*

[¶]*Department of Physics, University of Cambridge, J J Thompson Avenue, Cambridge CB3 0HE, United Kingdom*

[§]*Department of Chemistry, University of Surrey, Guildford GU2 7XH, United Kingdom*

^{||}*Institut Laue-Langevin, 71 Avenue des Martyrs, 38000 Grenoble, France*

E-mail: tamtoegl@gmail.com

1 Scientific background

In this experiment we measured the structure and diffusion of pyrazine ($C_4D_4N_2$ / $C_4H_4N_2$) on exfoliated graphite. The project builds upon our long-standing interest in the dynamics of hydrocarbons and small molecules on graphite⁴⁻⁷. By replacing some of the C atoms in benzene (C_6H_6) with N atoms (Figure 1), as done in the described measurements, experimental data can be compared to those with the structure and dynamics of aromatics having similar geometry, but different aromaticity and electronic structure.

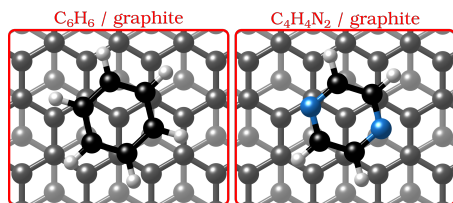


Fig. 1: The heterocyclic organic molecules benzene (C_6H_6) and pyrazine ($C_4H_4N_2$) adsorbed on graphite.

The introduction of N atoms into the ring reduces the electronic density around the carbon atoms of the molecule and decreases the repulsion between the π -orbitals of the ring and the substrate, giving rise to a stronger bonding to the substrate, because the intensity of the van-der-Waals (vdW) interactions is tuned by the polarisability and electrophilic character of the π -systems of the molecules interacting with the π -system of graphite¹⁻³. Benzene adsorbs in a flat (face-face) configuration on graphite and follows Brownian diffusion on this substrate as shown in previous neutron scattering experiments^{6,7}. Contrary to C_6H_6 , the behaviour of nitrogen containing heterocyclic compounds such as $C_4H_4N_2$ is much less understood, although previous theoretical studies confirm that, similarly to benzene, these N-containing molecules adsorb with a horizontal configuration¹.

2 Experimental details

Sample preparation As a substrate we used exfoliated compressed graphite, *Papyrus*, which exhibits an effective surface area of about $25 \text{ m}^2 \text{ g}^{-1}$ and retains a sufficiently low defect density^{14,15}. The prepared exfoliated graphite disks were heated to 973 K under vacuum before transferring them into a cylindrical aluminium sample cartridge. The amount of powder $C_4H_4N_2$ and $C_4D_4N_2$, required to reach the corresponding ML coverage, was weighed using a fine balance and then added to the graphite disks. The aluminium sample holders were hermetically sealed using a lid with a steel knife-edge. The samples were then heated in an evacuated furnace to 423 K to sublime the powder and promote its adsorption in the whole volume of the sample.

Instrumental details The measurements were carried out at the neutron time-of-flight (TOF) neutron spectrometer IN6-sharp and the high intensity neutron diffractometer D20 of the ILL¹⁶. Neutron diffraction measurements were carried out using a wavelength of $\lambda = 2.41 \text{ \AA}$. Data was taken in a range of momentum transfers $Q = |\mathbf{k}_f - \mathbf{k}_i| = (0, 0.51) \text{ \AA}^{-1}$ where \mathbf{k}_i and

\mathbf{k}_f are the neutron wavevectors before and after scattering from the sample, respectively. The TOF spectra were converted to scattering functions, $S(Q, \Delta E)$, where $Q = |\mathbf{Q}| = |\mathbf{k}_f - \mathbf{k}_i|$ is the momentum transfer and $\Delta E = E_f - E_i$ is the energy transfer.

3 Results

Neutron diffraction Measurements were performed at relative surface coverages of 0.9 and 1.5 ML of $C_4D_4N_2$, respectively, and at temperatures in the range 50 to 350 K. The temperature was controlled using a standard liquid helium cryostat (“orange” cryostat). Additional diffraction measurements of the clean graphite sample were performed at a number of temperatures. The graphite substrate and its orientation remained the same throughout all measurements.

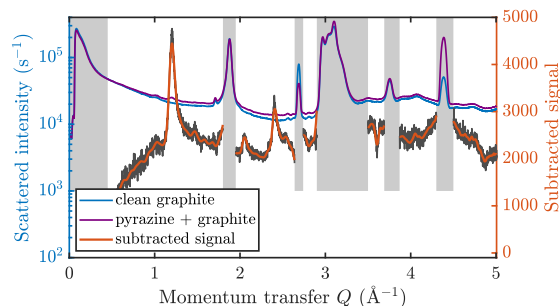


Fig. 2: Diffraction data at 300 K for the empty graphite sample and a coverage of 0.9 ML of $C_4D_4N_2$ together with the subtracted data. Regions with a strong graphite signal are indicated by a grey pattern. These regions are omitted in the subsequent analysis.

Subsequently, the clean graphite data was subtracted from the diffraction data of the adsorbate systems at equal temperature (Figure 2). Five regions in our data show very strong signal from the graphite substrate that masks the signal from the benzene adsorbate and makes a meaningful interpretation of the benzene signal impossible. These regions, as well as the low Q region, are marked by grey shading in Figure 2 and excluded in our further data analysis.

The temperature dependence of the subtracted signal, for both surface coverages is shown in Figure 3. While the subtraction procedure can still be improved, we carried a first analysis of the diffraction pattern out, based on simulated neutron diffraction patterns for a flat lying monolayer using the software package *npattern*. The software package allows to adjust a number of parameters manually¹⁷ and the peak positions obtained for a commensurate superstructure with lattice constants $a = b = 6.1 \text{ \AA}$ are shown as vertical dash-dotted lines in Figure 3.

The first analysis seems to be consistent with the model of a monolayer of densely packed and flat lying $C_4D_4N_2$ molecules in accordance to other heterocyclic organic molecules adsorbed on graphite. The lattice constant is significantly smaller compared to benzene ($a = b = 6.5 \text{ \AA}$ ¹⁸ and is in fact quite close to the constant of $a = b = 6.16 \text{ \AA}$ for 0.8 ML of s-triazine ($C_3H_3N_3$) on graphite, based on a X-ray diffraction study at room temper-

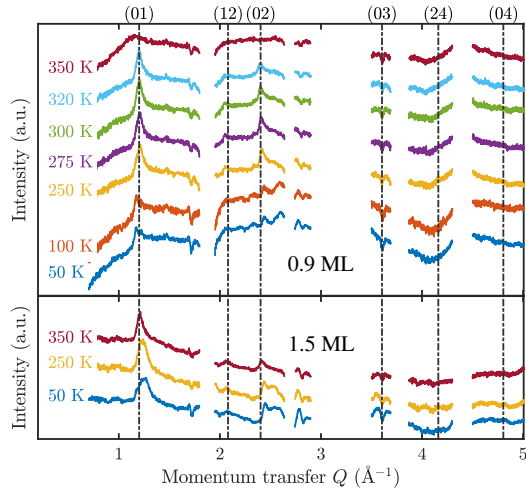


Fig. 3: Diffraction patterns for varying temperatures at a coverage of 0.9 ML $C_4D_4N_2$ (top panel) and 1.5 ML $C_4D_4N_2$ (bottom panel). The respective calculated peak positions for a commensurate monolayer with $a = b = 6.1 \text{ \AA}$ are shown by the vertical dash-dotted lines.

ature¹⁹. Thus we conclude that the unit cell size of the superstructure is similar to the one for s-triazine on graphite¹⁹ and the packing of $C_4D_4N_2$ is denser in comparison to benzene on graphite.

From Figure 3 it appears also that the bonding to the substrate is clearly stronger compared to benzene, with the superstructure peaks only vanishing at temperatures above room temperature while for benzene a melting starts to set in at 150 – 160 K¹⁸. Moreover it appears from the lower panel in Figure 3, that the superstructure persists above the monolayer thickness suggesting a layer by layer growth rather than the growth of a crystalline structure as observed for benzene¹⁸. Taken together the results suggest that indeed the introduction of nitrogen atoms into the ring increases the vdW bonding strength to the graphite substrate.

Neutron TOF Measurements were performed at relative surface coverages of 0.5 ML of $C_4H_4N_2$ at $T = 200, 270, 300, 330, 400, 435 \text{ K}$. The experimentally measured scattering function $S(Q, \Delta E)$ (normalised by Vanadium) was fitted using a convolution of the resolution function of the neutron TOF spectrometer $S_{res}(Q, \Delta E)$ (scattering function measured at base temperature) with an elastic term $I_{el}(Q)\delta(\Delta E)$, the quasi-elastic contribution $S_{inc}(Q, \Delta E)$ and a linear background:

$$S(Q, \Delta E) = S_{res}(Q, \Delta E) \otimes [I_{el}(Q)\delta(\Delta E) + A(Q) \frac{1}{2\pi} \frac{\Gamma(Q)}{[\Gamma(Q)]^2 + \Delta E^2} + C(Q)]. \quad (1)$$

Here, δ represents the Dirac delta and the quasi-elastic broadening is modelled by a Lorentzian function, where $I_{el}(Q)$ is the intensity of the elastic scattering and $A(Q)$ is the intensity of the quasi-elastic scattering. $\Gamma(Q)$ is the half width at half maximum (HWHM) of the Lorentzian.

Figure 4 shows the extracted quasi-elastic broadenings Γ versus momentum transfer Q upon fitting (1). There is evidence for two dynamic regimes / processes. It appears that for the 300 K data, Γ is almost constant with respect to Q which could e.g. be due to rotations of the molecule. Further analysis of the experimental data at 200 – 300 K is required to confirm the reliability/goodness of the fit and in order to provide a thorough analysis of the temperature behaviour.

From 330 – 400 K the broadening in Figure 4 shows a much clearer trend in terms of the momentum transfer dependence. The Arrhenius plot (Figure 5), extracted for the measurement at $Q = 1 \text{ \AA}^{-1}$ illustrates that at about 300 K an activated process seems to set in with an activation energy of about 80 meV.

Thus we conclude from a first preliminary analysis that the substitution of C atoms with N atoms in the benzene ring gives

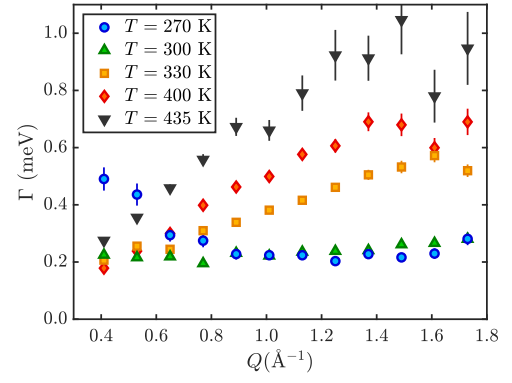


Fig. 4: Extracted quasi-elastic broadening $\Gamma(Q)$ for 0.5 ML $C_4H_4N_2$ at several temperatures versus momentum transfer Q .

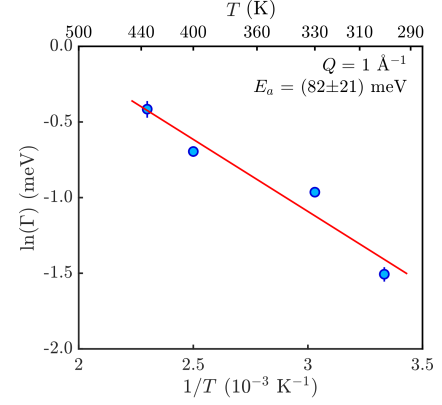


Fig. 5: Arrhenius plot for the extracted quasi-elastic broadening $\Gamma(Q)$ for 0.5 ML $C_4H_4N_2$ on graphite.

also rise to a different diffusive motion. The activated process starting to set in at about 300 K and probably related to the actual mass transport on the surface, appears at much higher temperatures compared to benzene diffusion (Refs.^{6,7}). After a more thorough analysis of the experimental data we expect to publish the results together with the vdW corrected DFT calculations in an international peer-reviewed publication.

1. Scott, A. M.; Gorb, L. *et al. J. Phys. Chem. C* **2014**, *118*, 4774–4783.
2. Zarudnev, E.; Stepanian, S. *et al. ChemPhysChem* **2016**, *17*, 1204–1212.
3. Zhang, Z.; Huang, H. *et al. The Journal of Physical Chemistry Letters* **2011**, *2*, 2897–2905.
4. Tamtögl, A.; Sacchi, M. *et al. Carbon* **2018**, *126*, 23–30.
5. Calvo-Almazán, I.; Sacchi, M. *et al. J. Phys. Chem. Lett.* **2016**, *7*, 5285–5290.
6. Calvo-Almazán, I.; Bahn, E. *et al. Carbon* **2014**, *79*, 183 – 191.
7. Hedgeland, H.; Fouquet, P. *et al. Nat Phys* **2009**, *5*, 561–564.
8. Wang, D.; Xu, Q.-M. *et al. Langmuir* **2002**, *18*, 5133–5138.
9. Martínez-Galera, A. J.; Gómez-Rodríguez, J. M. *J. Phys. Chem. C* **2011**, *115*, 11089–11094.
10. Dudde, R.; Frank, K.-H. *et al. Journal of electron spectroscopy and related phenomena* **1988**, *47*, 245–255.
11. Cervenka, J.; Budi, A. *et al. Nanoscale* **2015**, *7*, 1471–1478.
12. Tison, Y.; Lagoute, J. *et al. ACS Nano* **2015**, *9*, 670–678.
13. Chang, C.-H.; Fan, X. *et al. J. Phys. Chem. C* **2012**, *116*, 13788–13794.
14. Gilbert, E. P.; Reynolds, P. A. *et al. J. Chem. Soc. Faraday Trans.* **1998**, *94*, 1861–1868.
15. Finkelstein, Y.; Nemirovsky, D. *et al. Physica B Condens Matter* **2000**, *291*, 213 – 218.
16. Tamtögl, A.; Avidor, N. *et al. How does tuning the van der Waals bonding strength affect adsorbate structure and nanoscale diffusion?* Institut Laue-Langevin (ILL). doi:10.5291/ILL-DATA.7-05-496. 2019.
17. Brewer, A. Y.; Friscic, T. *et al. Mol. Phys.* **2013**, *111*, 73–79.
18. Bahn, E.; Hedgeland, H. *et al. Phys. Chem. Chem. Phys.* **2014**, *16*, 22116–22121.
19. Davidson, J. A.; Jenkins, S. J. *et al. Mol. Phys.* **2020**, *118*, e1706777.